Primary joint statistical seismic influence on ionospheric parameters recorded by the CSES and DEMETER satellites

Mei Li[1], Xuhui Shen[2], Michel Parrot[3], Chen Yu[4], Xuemin Zhang[5], Rui Yan[6], Dapeng Liu[7], Hengxin Lu[7], Feng Guo[7], and Jianping Huang[7]

[1]China Earthquake Networks Center
[2]Institute of Crustal Dynamics, CEA
[3]LPC2E/CNRS, Orleans, France
[4]China earthquake networks center
[5]Institute of Earthquake Forecasting, China Earthquake Administration
[6]Institute of Crustal and Dynamics, China Earthquake Administration
[7]Institute of Crustal Dynamics, China Earthquake Administration

November 28, 2022

Abstract

Oppositely to a previous statistical work using a single time resolution of the total ion density measured onboard the DEMETER satellite, this work deals with statistical seismo-ionospheric influences by comparing different parameters and various time resolutions. The O+ density and electron density recorded by the CSES satellite for more than one year and by the DEMETER satellite for about 6.5 years have been utilized to globally search ionospheric perturbations with different time resolutions. A comparison is automatically done by software between the occurrence of these ionospheric perturbations determined by different data sets, and the occurrence of earthquakes under the conditions that these perturbations occur at less than 1500 km and up to 15 days before the earthquakes. Combined with statistical results given by both satellites, it is shown that the detection rate r of earthquakes increases as the data time resolution and the earthquake magnitude increase and as the focal depth decreases. On average, the number of perturbations is higher the day of the earthquake, and then smoothly decreases the days before, which is independent of either ionospheric parameters or time resolutions. The number of right alarms is high near the South Atlantic Magnetic Anomaly area but its relationship with seismic activities is weak. The ion density tends to be more sensitive to seismic activities than the electron density but this needs further investigations. This study shows that the CSES satellite could effectively register ionospheric perturbations due to strong EQs as the DEMETER satellite does.

Primary joint statistical seismic influence on ionospheric parameters recorded by the CSES and DEMETER satellites

Mei Li[1], Xuhui Shen[2], Michel Parrot[3], Chen Yu[1], Xuemin Zhang[4], Rui Yan[2], Dapeng Liu[2], Hengxin Lu[2], Feng Guo[2], Jianping Huang[2]

[1]China Earthquake Networks Center, China Earthquake Administration, No.5, Sanlihe Nanhengjie, Xicheng District, 100045 Beijing, China
[2]The Institute of Crustal Dynamics, China Earthquake Administration, Beijing 100085, China
[3]Laboratoire de Physique et Chimie de l'Environnement et de l'Espace, Université d'Orléans, CNRS, 3A Avenue de la Recherche Scientifique, 45071 Orléans cedex 2, France
[4]Institute of Earthquake Forecasting, China Earthquake Administration, Beijing 100036, China

Correspondence to: M. Li (mei_seis@163.com)

Abstract. Oppositely to a previous statistical work using a single time resolution of the total ion density measured onboard the DEMETER satellite, this work deals with statistical seismo-ionospheric influences by comparing different parameters and various time resolutions. The O^+ density and electron density recorded by the CSES satellite for more than one year and by the DEMETER satellite for about 6.5 years have been utilized to globally search ionospheric perturbations with different time resolutions. A comparison is automatically done by software between the occurrence of these ionospheric perturbations determined by different data sets, and the occurrence of earthquakes under the conditions that these perturbations occur at less than 1500 km and up to 15 days before the earthquakes. Combined with statistical results given by both satellites, it is shown that the detection rate *r* of earthquakes increases as the data time resolution and the earthquake magnitude increase and as the focal depth decreases. On average, the number of perturbations is higher the day of the earthquake, and then smoothly decreases the days before, which is independent of either ionospheric parameters or time resolutions. The number of right alarms is high near the South Atlantic Magnetic Anomaly area but its relationship with seismic activities is weak. The ion density tends to be more sensitive to seismic activities than the electron density but this needs further investigations. This study shows that the CSES satellite could effectively register ionospheric perturbations due to strong EQs as the DEMETER satellite does.

1 Introduction

With the development of Earth observation satellites, their onboard experiments have gradually shown their potential application in the field of earthquake (EQ) monitoring and investigation. This is due to their advantages of fast-speed, large-scale and high-resolution results, especially for areas with harsh natural conditions. On one hand, scientific data from satellites have been utilized to distinguish precursors prior to strong EQs. As one result of researches during the last ten years, it has been shown that the ionosphere is unexpectedly sensitive to the seismic activity [*Hayakawa and Molchanov*, 2002]. On the other hand, these satellite data have also been combined with ground-based observations to study the lithosphere-atmosphere-ionosphere coupling [*Pulinets et al.*, 1994, 1997, 2000; *Hayakawa and Molchanov*, 2002; *Molchanov et al.*, 2004; *Molchanov and Hayakawa,* 2008; *Pulinets and Ouzounov*, 2011; *Sorokin et al.*, 2015; *Li et al.*, 2016, 2019; and references therein].

Irregularities in the ionospheric sounder data before the Alaskan earthquake taking place on March 28, 1964 were reported as early as 1965 [*Davies and Baker*, 1965]. However, examples have been recently intensively reported about seismic influence on different ionospheric parameters as modern satellite-borne receivers develop, especially after the launch of the DEMETER (Detection of Electro-Magnetic Emissions Transmitted from Earthquake Regions) satellite in 2004 in France. Ionospheric variations have been confirmed before the L'Aquila M_S 6.2 EQ on 6 April 2009 on GPS TEC (Total Electron Content) and DEMETER IAP (Instrument d'Analyse du Plasma) ion density and ISL (Instrument Sonde de Langmuir) electron density [*Akhoondzadeh et al.*, 2010; *Stangl et al.*, 2011]. Notably, multi-parameter ionospheric changes have also been reported prior to the huge Wenchuan M_S 8.0 EQ on 12 May 2008 including (i) the f0F2 (critical frequency of the F2 layer) values measured by ground–based sounders, and the VLF fields [*Zhao et al.*, 2008; *Yu et al.*, 2009; *Ding et al.*, 2010; *Xu et al.*, 2010a, b; *Xu et al.*, 2011; *Sun et al.*, 2011; *Maurya et al.*, 2013], (ii) the ion density, electron density, electron temperature, ULF (Ultra Low Frequency), VLF and and ELF (Extremely Low Frequency) electric fields, O+ density, ion temperature, and energetic particle measured by DEMETER [*Akhoondzadeh et al.*, 2011; *Zhang et al.*, 2009a, b; *Zeng et al.*, 2009; *An et al.*, 2010; *BŁEÇKI et al.*, 2010; *Sarkar et al.*, 2010; *He et al.*, 2011a, b; *Onishi et al.*, 2011; *Yan et al.*, 2012; *Wan et al.*, 2012; *Walker et al.*, 2013; *Ryu et al.*, 2014; *Liu et al.*, 2015], (iii) the TEC measured by GPS satellites [*Akhoondzadeh et al.*, 2011; *Pulinets and Ouzounov*, 2011; *Zhao et al.*, 2008; *Yu et al.*, 2009; *Yan et al.*, 2012; *Ryu et al.*, 2014; *Zhao et al.*, 2010; *Lin et al.*, 2009; *Liu et al.*, 2009; *Zhu et al.*, 2009; *Pulinets et al.*, 2010; *Ma et al.*, 2014], (iv) the TEC and NmF2 (electron density at F2 peak) values measured by radio occultation using the six microsatellites FORMOSAT3/COSMIC (F3/C) [*Liu et al.*, 2009; *Ma et al.*, 2014; *Hsiao et al.*, 2010], and (v) the electron density measured by the CHAMP satellite [*Ryu et al.*, 2014]. This shows that various ionospheric parameters measured by several scientific payloads onboard a satellite can response to a seismic event, especially for strong EQs.

There has been many statistical works on ionospheric variations associated with strong seismic events using satellite measurements. Seismo-ionospheric disturbances within a few days before EQs have been registered in 73% of EQs with magnitude 5.0, and in 100% of EQs with magnitude 6.0 [*Pulinets*, 2003]. *Liu et al.* [2009] have performed a statistical analysis on GPS TEC and found that seismo-ionospheric variations above the epicentral area occurred 5 days prior to 16 EQs out of 20 events with $M \geq 6.0$ in the Taiwan area from September 1999 to December 2002. Statistical analyses have also been performed using DEMETER data sets. A statistically significant decrease of wave intensity at 1.7 kHz during nighttime four hours before the occurrence of EQs has been reported respectively by *Němec et al.* [2008, 2009] and by *Píša et al.* [2012, 2013]. Statistical analyses have been performed using a total ion density (the sum of H^+, He^+ and O^+) data set during the DEMETER lifetime (6.5 years) in the epicenter areas of earthquakes as well as in their magnetically conjugate point areas and the results have showed a significant statistical correlation between ionospheric anomalies and large events within a few days before the events [*Parrot*, 2011, 2012; *Li and Parrot*, 2012, 2013, 2018; *Parrot and Li*, 2017; *Yan et al.*, 2017]. *Zhang et al.* [2013] have found that there are increases in the number of electron bursts prior to strong EQs with a magnitude over 7.0 during the entire operation period of the DEMETER satellite. However, *Akhoondzadeh et al.* [2010] statistically analyzed the ionospheric variations prior to four large EQs simultaneously using on one hand, several satellite parameters of DEMETER: IAP ion density and ion temperature, ISL electron density and electron temperature, and on the other hand, GPS TEC. Their results show that there is a very good agreement between the different parameters and that, positive and negative anomalies appeared 1 to 5 days before all studied EQs during quiet geomagnetic conditions, although their amplitude depends on the magnitude of the EQs involved.

CSES satellite has been launched for more than one year and effective payload data have been recorded. It is possible to check its response to seismic activities during this period. So, in this paper, a primary statistical analysis on seismo-ionospheric influence of different parameters of ion density and electron density recorded by CSES and DEMETER satellites will be comparatively shown. The CSES satellite and DEMETER satellite are briefly described in section 2. In section 3, the data processing method is retrospectively introduced. In section 4, automatic statistical results for different parameters recorded by CSES will be compared with that of DEMETER and confirmed. Discussion and conclusions are provided in section 5.

2 The CSES satellite and the DEMETER satellite

The China Seismo-Electromagnetic Satellite (CSES) was launched successfully on 2 February 2018. The CSES is a Sun-synchronous satellite orbiting at a height of 500 km with a descending node of 14:00 local time (LT). There are eight scientific payloads onboard, including a search-coil magnetometer, an electric field detector, a high precision magnetometer, a plasma analyzer package, a Langmuir probe, an energetic particle detector, a GNSS occupation receiver, and a three-frequency beacon. Of these, the Langmuir probe (LAP) and plasma analyzer package (PAP) are the space plasma in-situ detection payloads. Their scientific design parameters can be referred to [*Shen et al.*, 2018; *Yan et al.*, 2018; *Liu et al.*, 2018]. The LAP allows access to the electron density and temperature. The operational modes of the LAP include survey mode and burst mode. The survey mode is used mainly to detect global electron density and electron temperature with sweeping period of 3 s (second), while the burst mode primarily allows detection of key areas, over China and within global main seismic belts with sweeping period of 1.5 s. The PAP measures ion density, composition, temperature, and flow velocity. PAP has also the same operational modes as that of LAP but with a little higher resolution of 1 s for survey mode and 0.5 s for burst.

DEMETER was launched in June 2004 onto a polar and circular orbit which measures electromagnetic waves and plasma parameters all around the globe except in the auroral zones [*Parrot*, 2006]. DEMETER is a low-altitude satellite with an altitude of 710 km, which was decreased to 660 km in December 2005. The orbit of DEMETER is nearly sun-synchronous and the up-going half-orbits correspond to night time (22.30 LT) whereas the down-going half-orbits correspond to day time (10.30 LT). The onboard experiments of DEMETER includes six scientific payloads, the IAP-plasma analyser instrument, the ICE-electric field instrument, the ISL-Langmuir probe, the IMSC-search-coil magnetometer instrument, the IDP-particle detector instrument and the BANT-an electronic unit. The variations of the ion density and the electron density are measured by the instrument IAP and ISL, respectively. These two experiments have different operational modes. The ISL is with an experimental resolution of 1 s for all data, while the IAP has two experimental data resolutions of 4 s in survey mode and 2 s in burst mode. Details of the IAP and ISL experiments can be found in *Berthelier et al.* [2006] and *Lebreton et al.* [2006]. The satellite's science mission has come to an end in December 2010.

3 Description of the data processing

3.1 Data

The O^+ is the main ion among the ions H^+, He^+ and O^+ detected by the satellites and it stands for more than 85% of the total ion density. So, the used data of CSES satellite include PAP O^+ density and LAP electron density from 1 August 2018 to 30 November 2019. During this period, 4317 strong EQs with magnitudes M_W equal to or more than 4.8 occurred (USGS: http://www.usgs.gov).

The DEMETER data used here include the completed data for the parameter IAP O^+ density and ISL electron density covering its lifetime from the mid 2004 to the end 2010. During this period (6.5 years in total) there are 21863 strong EQs with magnitude $M_W \geq 4.8$ which took place (USGS: http://www.usgs.gov).

The Kp index (http://isgi.unistra.fr) is also checked in order to avoid the effect from the solar activities during all the periods considered in this paper.

3.2 Data processing method

The data processing method here is similar to the one used before by *Li and Parrot* [2012, 2013]. First of all, a software is used to automatically search global ionospheric perturbations in several data sets (issued from CSES or DEMETER). Only the perturbations which comply with the duration time between 20 and 120 seconds are kept in the perturbation database. The information for each perturbation in the perturbation database includes peak appearing time, orbit number, location (latitude and longitude), background value, amplitude, change trend (increase or decrease; if the amplitude is larger than the background value, it is increase, if not, it is decrease), increase or decrease percentage, duration time and extension distance (km).

In order to examine the capability of recording seismic influence on the ionosphere with different data time resolutions using our software, the raw data are sampled at different time resolutions: 1 s and 3 s for PAP O+ density and 3 s for LAP electron density of CSES; 4 s for IAP O+ density and 3 s and 4 s for ISL electron density of DEMETER. Thus six data sets have been established: PAP-1 s, PAP-3 s and LAP-3 s for CSES; IAP-4 s, ISL-3 s and ISL-4 s for DEMETER. At the same time, the SAVGOL method is employed to smooth the data before searching for perturbations. The SAVGOL function returns the coefficients of a Savitzky-Golay smoothing filter [*Savitzky and Golay*, 1964]. So, at this stage, two O+ perturbation databases (1 s and 3 s data are used respectively) and one electron database (3 s data) for CSES, and one O+ perturbation database (4 s data) and two electron databases (3 s and 4 s data) for DEMETER have been established.

After, a second software is used to check whether the ionospheric perturbations are corresponding to an EQ or not under the following three limits, (i) the Kp index is kept to be less than 3 in order to reduce the effect of the geomagnetic activity on the ionosphere. This geomagnetic activity is induced by solar magnetic storms, (ii) the distance (*D*) between the location of the perturbation on the orbit and the epicentre is equal to or less than 1500 km, and (iii) the delay time (*T*) before an EQ is equal to or less than 15 days. If an earthquake is corresponding to one or to more than one perturbation, we consider it is a good detection; if not, it is a bad detection. If a perturbation corresponds to an earthquake, it is a right alarm; if not, it is a false alarm. More details can also be found in *Parrot and Li* [2017] and *Li and Parrot* [2018].

An example of ionospheric perturbation detected by the software and corresponding to an EQ is shown in Figure 1. It corresponds to an EQ occurring on August 21, 2018 at 21:31:47 UT with a magnitude equal to M_W 7.3 and a depth equal to 147 km. Its position was 10.77 °N, 62.90 °W. Figure 1a shows variations of PAP parameters. From the top to the bottom, the panels show the densities of the H^+, He^+, and O+ ion. The X-axis represents UTC (Universal Time Coordinated)/BJT (Beijing time), Latitude, Longitude and Altitude of CSES satellite. At 6:00 UT, about 15 hours before this EQ, the orbit 03040 flew up this epicentral area and an increase of O^+ labelled by a black arrow in the bottom panel with red curve is observed in Figure 1a (this variation seems not obvious at this period because of high values in high latitude. Correspondingly, the payload LAP also recorded clear increase of electron density on the same orbit as it is shown in the bottom panel with a black arrow in Figure 1b.

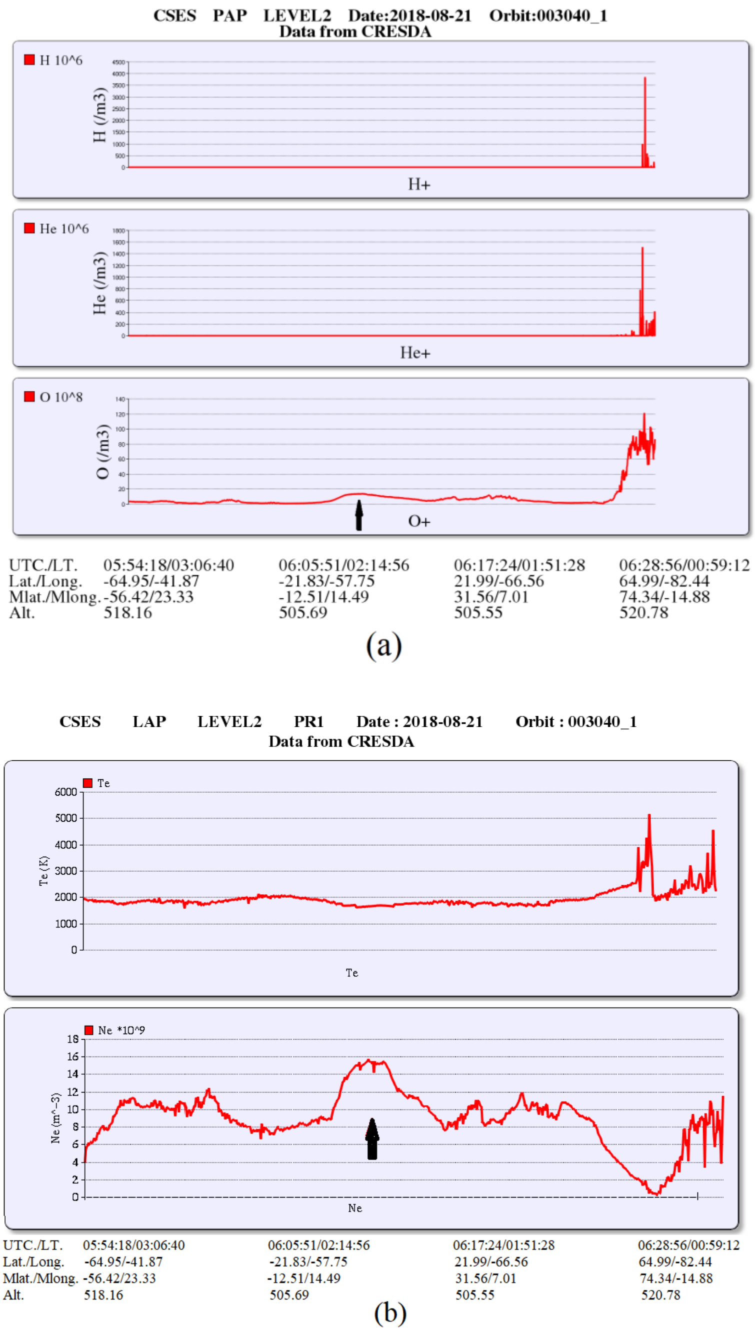

Figure 1. Data recorded on 21 August 2018 between 05:54:18 UT and 06:28:56 UT, 15 h before a M_W 7.3 EQ along the orbit 03040_1. (a) Variations of ion densities recorded by PAP onboard the CSES satellite. The panels from the top to the bottom are H^+ density, He^+ density, and O^+ density. An increase has been labeled by a black arrow in O^+ curve and it looks not obvious because of large scale of Y-axis coordinate. In fact, the automatic detection indicates that this increase amplitude is about 29%. (b) Variations of electron data recorded by LAP onboard the CSES satellite. The top panel is the electron temperature (Te) and the bottom one is the electron density (Ne) with an apparent 21.9% increase labeled by a black arrow. The parameters below the plots indicate the time in UT/LT and the position of the satellite along its orbit.

These two ionospheric perturbations of PAP and LAP have been successfully detected by the software and their information is shown in Table 1. From Table 1, one can see that these two ionospheric perturbations almost occurred at the same time, and then the two peaks have a very near location (477 km and 483 km away from the epicentre of this M_W7.3 EQ). The corresponding increases relatively to the background values are larger than 20%.

Table 1. Information on the PAP ion density and the LAP electron density perturbations shown in Figure 1 and automatically detected by the software.

PAP O^+ density perturbation	LAP electron density perturbation
Time: 2018 8 21 6 15 31 712	Time: 2018 8 21 6 15 26 856
Orbit: 3040	Orbit: 3040
Suborbit: 1	Suborbit: 1
Latitude: 14.5951	Latitude: 14.5468
Longitude: -65.0325	Longitude: -65.0051
BkgdIon (/m^3): 336.602	BkgdElectron (/m^3): 8473.04
Amplitude (/m^3): 434.302	Amplitude (/m^3): 10332.1
Trend: Increase	Trend: Increase
Percent: 29.0254	Percent: 21.9409
Time_width (m s ms): 1 27 1	Time_width (m s ms): 1 57 0
Extension (km): 619.000	Extension (km): 837.000

4 Statistical seismo-ionospheric influences

4.1 EQ detection rate

Here, a parameter r is defined as the EQ detection rate, which is the ratio of the number of EQs detected and the number of EQs which comply with the limit conditions given above.

EQs are still divided into different groups during this work in order to gain an easy comparison as properties of EQs vary. The 4317 $M_W \geq 4.8$ EQs occurring between August 2018 and November 2019 as CSES satellite flies, have been divided into three groups according to their magnitudes: $4.8 \leq M_W \leq 5.0$ 2524 EQs, $5.0 < M_W \leq 6.0$ 1624 EQs and $M_W > 6.0$ 169 EQs. Then, in light of previous statistical seismo-ionospheric influences for EQs located in different areas of the world (see for example the effect of the South Atlantic Magnetic Anomaly (SAMA) on EQ detection reported by *Li and Parrot* [2012, 2013]), two specific rectangular zones have been selected (see Figure 6 in Section 5), (i) a Zone1 with latmin = -70 °, latmax = -45 °, longmax = 150 °W, longmin = 20 °W, which lies in the SAMA area in south hemisphere and includes 190 EQs, and (ii) a Zone2 with latmin = 0 °, latmax = 30 °, longmin = 90 °E, longmax = 150 °E, which lies in low-mid latitude in north hemisphere and includes 774 EQs. For each group of EQs, they are detected under the conditions of D = 1500 km, T = 15 d and the focal depth d = 0–1000 km with different ionospheric databases confirmed by data sets of PAP-1 s and PAP-3 s data and LAP-3 s from CSES. To check effects of the focal depth (d) of earthquakes on the detection rate, "crust" earthquakes with d

≤ 20 km have been comparatively detected for each group of EQs. The Kp index is kept to be less than 3 during this period in order to eliminate the effect from solar activities. Their corresponding detection rates are listed in Table 2.

Table 2. Detected rates *r* for different groups of EQs and different data sets (PAP-1 s, PAP-3 s and LAP-3 s) recorded by CSES (D = 1500 km, T = 15 days).

		$4.8 \le M \le 5.0$	$5.0 < M \le 6.0$	$M > 6.0$	Zone1	Zone2
Data set	*d*	*r*	*r*	*r*	*r*	*r*
PAP-1 s	0–1000	54.5%	61.1%	89.9%	63.2%	46.4%
	0–20	64.1%	67.5%	87.0%	66.4%	50.1%
PAP-3 s	0–1000	45.4%	53.1%	87.6%	56.8%	35.0%
	0–20	56.3%	61.3%	87.0%	59.4%	50.0%
LAP-3 s	0–1000	45.4%	51.5%	85.2%	61.1%	42.0%
	0–20	56.4%	59.7%	84.4%	67.2%	46.6%

From Table 2, except $M > 6.0$ with contrary result due to its less examples (169 in total and 77 with the depth $d \le 20$ km), the detection rate *r* for "crust" EQs with d = 0 – 20 km is thoroughly higher than that of EQs with d = 0 – 1000 km for each group of EQs in all data sets. These results tend to verify a definite conclusion that ionospheric influence can be affected by the epicentre depth: the "crust" EQs can be easily detected than "deep" ones, which has been already reported by *Li and Parrot* [2012] and *Silina et al.* [2001].

For a better comparison, the data in Table 2 with d = 0–1000 km have been shown in Figure 2 under the form of histograms.

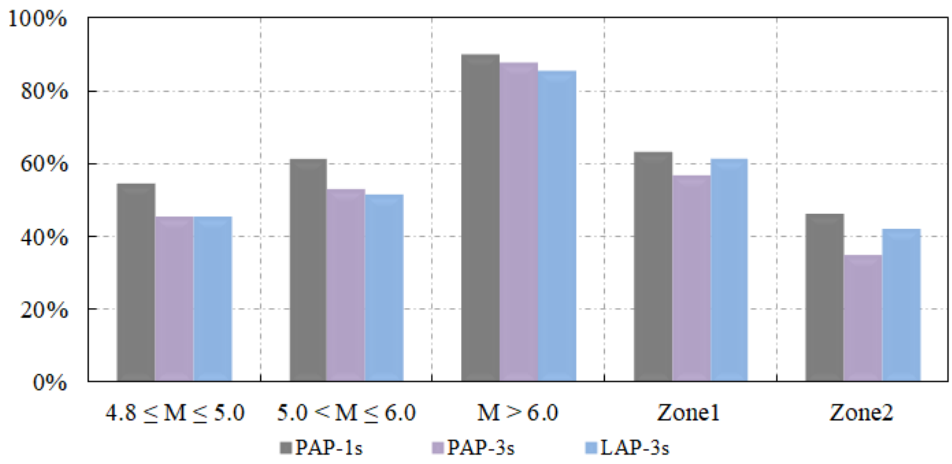

Figure 2. Histogram of EQ detection rates for different groups of EQs: $4.8 \le M \le 5.0$, $5.0 < M \le 6.0$, $M > 6.0$, Zone1 and Zone2. Each group of EQs are detected under the conditions of D = 1500 km, T = 15 d and the focal depth d = 0–1000 km with different ionospheric databases confirmed by data sets of PAP-1 s and PAP-3 s data and LAP-3 s from CSES. The time period is from August 2018 to November 2019 as CSES flies.

From Table 2 and Figure 2, on one hand, it is clear that the detection rate r increases as the magnitude of EQs increases. On the other hand, for the same parameter PAP O^+ density with different data time resolutions of 1 s and 3 s, the detection rates of PAP-1 s for six group EQs of $4.8 \leq M_W \leq 5.0$, $5.0 < M_W \leq 6.0$, $M_W > 6.0$, Zone1 and Zone2 are higher than that of PAP-3 s, which means that the detection rate r increases as the time resolution of data increases; for different parameters of PAP O^+ density and LAP electron density with the same time resolution of 3 s, detection rates of PAP for $4.8 \leq M_W \leq 5.0$, $5.0 < M_W \leq 6.0$ and $M_W > 6.0$ groups of EQs tend to be all higher a little than that of LAP but this law are contrary for the two group EQs of Zone1 and Zone2.

In order to confirm the results given by CSES, the 21863 EQs occurring during the DEMETER 6.5 year life time, have been classified into six groups of EQs: $4.8 \leq M_W \leq 5.0$ 12057 EQs, $5.0 < M_W \leq 6.0$ 8953 EQs, $M_W > 6.0$ 853 EQs, Zone1 [70 °S, 45 °S] [150 °W, 20 °W] 615 EQs and Zone2 [0 °N, 30 °N] [90 °W, 150 °W] 4549 EQs. They are also detected with the same software under the conditions of D = 1500 km, T = 15 d, and d = 0–1000 km and Kp < 3 with the different ionospheric perturbation databases named IAP-4 s, ISL-3 s and ISL-4 s (see section 3.2) . Their corresponding detection rates r are listed in Table 3.

Table 3. Detected rates for different groups of EQs and different time resolutions of perturbations recorded by DEMETER (D = 1500 km, T = 15 days, d = 0–1000 km).

	$4.8 \leq M \leq 5.0$	$5.0 < M \leq 6.0$	$M > 6.0$	Zone1	Zone2
Data set	r	r	r	r	r
ISL-3 s	37.3%	43.0%	68.3%	65.7%	11.8%
ISL-4 s	31.0%	36.7%	57.9%	58.7%	9.4%
IAP-4 s	49.5%	55.1%	76.7%	63.4%	17.0%

For a better comparison, the data of Table 3 is shown in Figure 3 under the form of histograms.

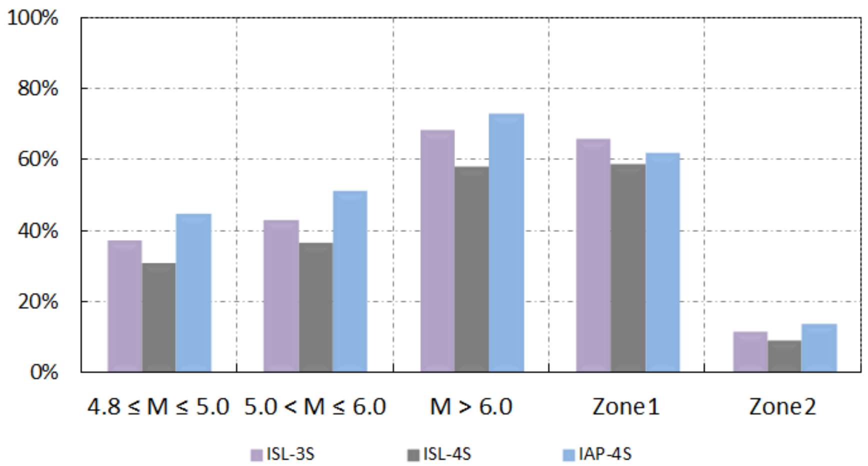

Figure 3. Histogram of detection rates using different time resolution data of IAP 4 s and ISL 3 s and 4 s recorded by DEMETER for different groups of EQs: $4.8 \leq M_W \leq 5.0$, $5.0 < M_W \leq 6.0$, $M_W > 6.0$, Zone1 and Zone2. The time period corresponds to the lifetime of DEMETER.

From Table 3 and Figure 3, one thing we can reconfirm is that the detection rate r increases as the time resolution of the same ionospheric parameter ISL electron density increases.

Another point is that the detection rates for IAP density are clearly higher than that of ISL density for each group of EQs when the time resolution is the same, which probably gives a conclusion that the ion density is more sensitive to seismic activities than the electron density although this claim is not completely verified by the CSES data.

4.2 Temporal evolution of seismo-ionospheric influences

To check the occurrence frequency of ionospheric perturbations during EQ preparation, a study has been conducted on the different cases, and the corresponding results are shown in Figure 4. Figure 4 displays the number of detected perturbations corresponding to an EQ (right alarms) as a function of days before the good detections considering the following data sets recorded by CSES: All EQs (4317 EQs), $4.8 \leq M_W \leq 5.0$ EQs, Zone1, and Zone2. In each panel of Figure 4 the results are expressed as a percentage relative to the total number of right alarms detected by PAP-1 s (red line), PAP-3 s (blue line) and LAP-3 s (orange line) data sets. In a similar way, Figure 5 is related to DEMETER and displays the relative percentage each day before, considering: All EQs (21863 EQs), $4.8 \leq M_W \leq 5.0$ EQs, Zone1, and Zone2. Each panel shows three percentage lines determined by the ISL-3 s (red line), ISL-4 s (blue line) and IAP-4 s (orange line) data sets.

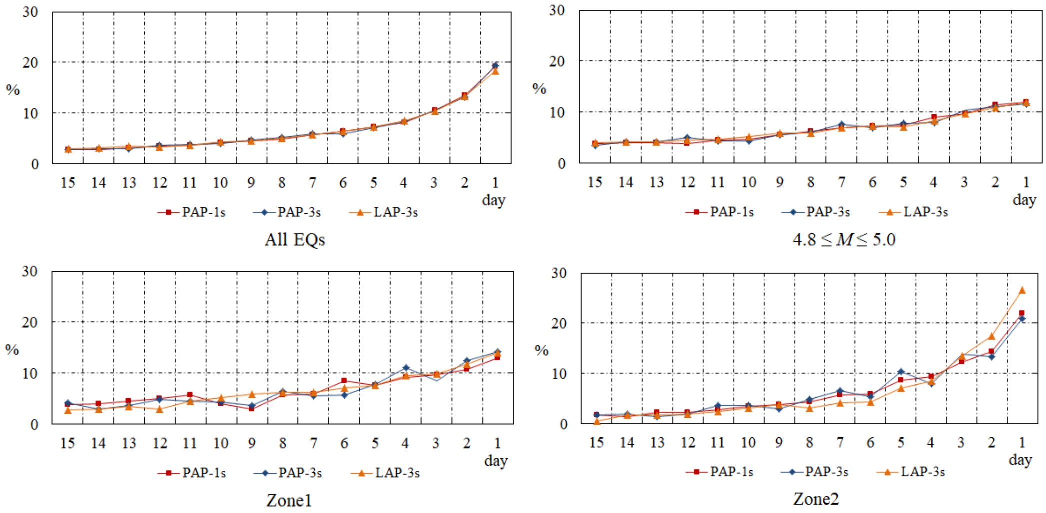

Figure 4. Variation of the number of perturbations as a function of the days before the EQs and for different cases (top left: all detected EQs, top right: detected EQs of $4.8 \leq M_W \leq 5.0$, bottom left: detected EQs in Zone1, bottom right: detected EQs in Zone2). Each panel covers three groups of seismo-ionospheric influences determined by PAP-1 s (red line), PAP-3 s (blue line) and LAP-3 s (orange line) data sets recorded by CSES.

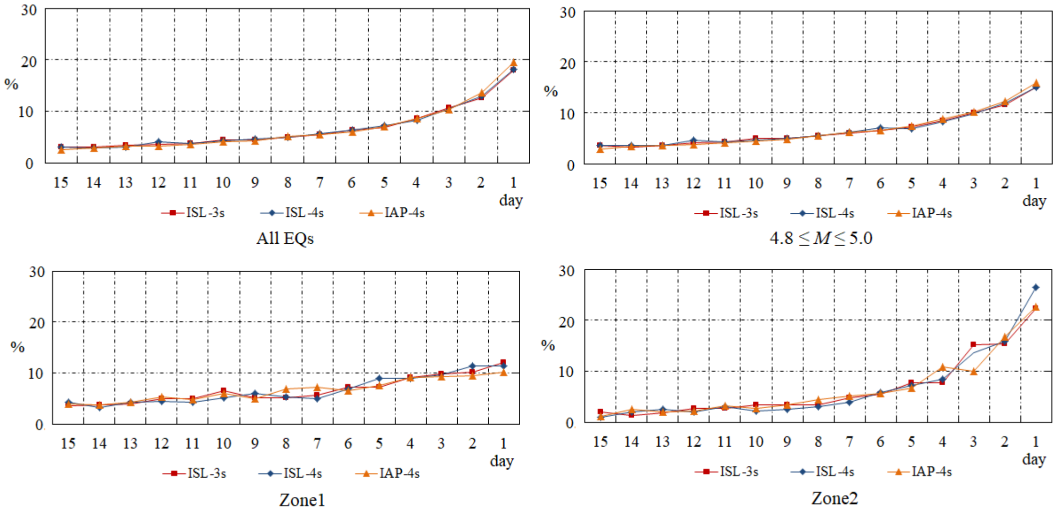

Figure 5. Variation of the number of perturbations as a function of the days before the EQs and for different cases (top left: all detected EQs, top right: detected EQs of $4.8 \leq M_W \leq 5.0$, bottom left: detected EQs in Zone1, bottom right: detected EQs in Zone2). Each panel covers three groups of seismo-ionospheric influences determined by ISL-3 s (red line), ISL-4 s (blue line) and IAP-4 s (orange line) data sets recorded by DEMETER.

It can be seen that, for all cases in Figure 4 and Figure 5, the number of perturbations is maximum for days close to the EQ day and smoothly decreases when the time before the EQ is increasing. This is a variation that is intuitively expected. On one hand, this variation seems not mainly affected by the data time resolution of a given parameter whatever this parameter is. On the other hand, this trend becomes more obvious when the number of samples is large enough. Thus, three lines decay smoothly as day goes for All EQs (see the top left panel in Figure 4 and Figure 5) but with a few fluctuations for other cases (see other panels also in Figure 4 and Figure 5). However, the percentages increase more obviously in Zone2 (see the bottom right panel in Figure 4 and Figure 5) than in Zone1 especially one week before the EQs. This means that the perturbations have a little relationship with seismic activity in the Zone1 area. In this case, false alarms become more important due to outer disturbances of the active E×B drift occurring in the South Atlantic Magnetic Anomaly [*Abdu et al.*, 1977, 2003, 2005].

5 Discussion and conclusions

As CSES satellite has run more than one year since it was launched on February 2, 2018 in China, this increases the probability to examine the effectiveness of seismo-ionospheric influences recorded by the scientific payloads of PAP O^+ density and LAP electron density. For comparison, two corresponding DEMETER parameters of IAP and ISL for about 6.5 years have also been check to gain some similar results.

Oppositely to previous statistical works with DEMETER using a single time resolution of one parameter of IAP total ion density [*Li and Parrot*, 2012, 2013], this work is associated with statistical seismo-ionospheric influences using two parameters recorded by the DEMETER and CSES satellites, respectively. At the same time, various time resolutions for a given parameter are also employed to survey the effects of seismic activities on the ionosphere, but also to check the efficiency of our two software.

Numerous investigations have shown that ionospheric variations generally appeared several days to two weeks prior to EQs. However, the abnormal range in the ionosphere arise from seismic activities has not been well established so far. The software in this paper is designed to only accept ionospheric perturbations with a duration of 20–120 s (about 160–840 km if the speed of the satellite 7.0 km/s is considered.) and positive results have been given. In order to further examine this design is effective for the investigations, variations with a duration of 200–300 s using PAP-1s data set from August 1 2018 to November 30 2019 have been accepted this time and 509 ionospheric perturbations have been attained in total. These perturbations are located in the map of the world (see Figure 6 with purple dots). As a comparison, a global ionospheric plasma variation has been given by O+ ion density recorded by CSES satellite during this period and the main seismic zones in the world are basically determined by 4317 EQs occurred during this period, which cover especially plate-boundary interfaces, Circum-Pacific seismic belt, and Chile seismic zone (black dots in Figure 6). Zone1 and Zone2 employed above in Section 4 are also added to Figure 6 by two black empty rectangles.

From Figure 6, it is clear that these perturbations collect mainly around the equator. This distribution is not coincident with the main seismic belts of the world, but keeps the similar shape as the background distribution of ion density. These large-scale ionospheric dynamical variations near the equator have been formed arise from some complex origins, such as Equatorial plasma bubbles, which are extremely dynamical phenomena with density drop out more than an order of magnitude over distances of a few kilometers perpendicular to the magnetic field leading to large-scale ionospheric variations [*Berthelier et al.*, 2006]. At higher latitudes, more intense waves are characterised by auroral emissions duo to strong sources of ELF/VLF emissions [*Lefeuvre et al.*, 1992].

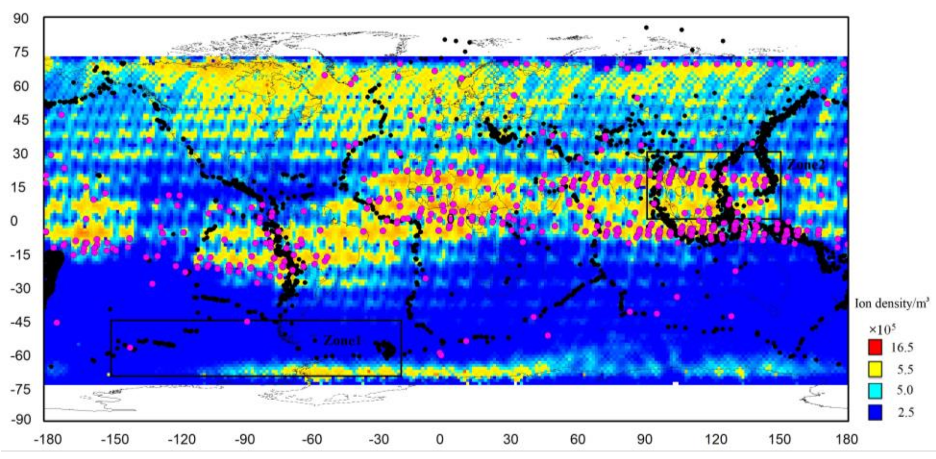

Figure 6. Distribution of large-scale ionospheric perturbations with a duration of 200–300 s (purple dots) automatically searched by software using PAP-1s data set from August 1 2018 to November 30

2019. Here, O^+ ion density recorded by CSES satellite during October to December 2018 stands for a global ionospheric plasma variation. The main seismic zones in the world are basically determined by 4317 EQs occurred during this period (black dots). Zone1 and Zone2 used above in Section 4 have been labeled by two black empty rectangles.

The results show that the detection rate *r* could be affected by the data time resolutions because high time resolution data can record small scale ionospheric variations. Thus the detection rate tends to increase as the time resolution increases. For the same time resolution, the detection rate *r* determined by IAP O^+ density for all cases are always higher than that of ISL electron density on DEMETER (see Table 3 and Figure 3), but these results gained partly on CSES (see Table 2 and Figure 2) probably owing to a less number of samples. However, there are still a high false alarm number and a high bad detection number due to the fact that a single satellite cannot continuously survey a given area, and then the natural disturbances of the ionosphere. Thus, it seems that EQs in SAMA zone have a higher detection rate but the right alarms have a weak relationship to seismic activities (see bottom left panels in Figure 4 and Figure 5).

However, overall the results given by CSES and DEMETER have shown that

– The CSES ionospheric data can effectively respond to strong EQs.

– The detection rate *r* increases as the time resolution of the satellite data and the magnitude of EQs involved increase and decreases as the epicentral depth of seismic events increases.

– On average, the occurring frequency of perturbations is higher the day of the EQ and then gradually decreases before the event. This is independent of the data sets we use, either the ion density or the electron density, and whatever are their time resolutions.

– The ion density seems to be more sensitive to the seismic activities than the electron density but it needs further investigations with more data.

Acknowledgments

This work uses data from the CSES mission, a project funded by the China National Space Administration (CNSA) and the China Earthquake Administration (CEA). This work was also supported by the Centre National d'Etudes Spatiales. It is based on observations with the plasma analyzer IAP and the Langmuir probe ISL embarked on DEMETER. This work was supported by the National Key R&D Program of China under Grant No. 2018YFC1503506 and the National Natural Science Foundation of China (NSFC) under Grant No. 41774084. The data utilized in this paper are available through the website http://www.leos.ac.cn/.

References

Abdu, M. A., and I. S. Batista (1977), Sporadic E-layer phenomena in the Brazilian magnetic anomaly: Evidence for a regular particle ionization source, *J. Atmos. Terr. Phys*., *39*, 723–732, doi:10.1016/0021-9169(77) 90059-9.

Abdu, M. A., J. W. MacDougall, I. S. Batista, J. H. A. Sobral, and P. T. Jayachandran (2003), Equatorial evening pre-reversal electric field enhancement and sporadic E layer disruption: A manifestation of E and F region coupling, *J. Geophys. Res.*, *108*(A6), 1254, doi:10.1029/ 2002JA009285.

Abdu, M. A., I. S. Batista, A. J. Carrasco, and C. G. M. Brum (2005), South Atlantic magnetic anomaly ionization: A review and a new focus on electrodynamic effects in the equatorial ionosphere, *J. Atmos. Sol. Terr. Phys.*, *67*, 1643–1657, doi:10.1016/j.jastp.2005.01.014.

Akhoondzadeh, M., M. Parrot, and M. R. Saradjian (2010), Electron and ion density variations before strong earthquakes (M > 6.0) using DEMETER and GPS data, *Nat. Hazards Earth Syst. Sci.*, *10*(1), 7–18, doi: 10.5194/nhess-10-7-2010.

An, Z., Y. Fan, J. Liu, D.Tan, J. Chen, G. Zheng, and T. Xie (2010), Analysis on ion temperature variation detected by DEMETER before 2008 Wenchuan M_S 8.0 earthquake, *Acta Seismologica Sinica, 32*(6), 754–759 (in Chinese with English abstract).

Berthelier, J. J., M. Godefroy, F. Leblanc, E. Seran, D. Peschard, P. Gilbert, and J. Artru (2006), IAP, the thermal plasma analyzer on DEMETER, *Planet. Space Sci.*, *54*, 487–501, doi:10.1016/j.pss.2005.10.018.

BŁEÇKI, J., M. Parrot, and R. Wronowski (2010), Studies of the electromagnetic field variations in ELF frequency range registered by DEMETER over the Sichuan region prior to the 12 May 2008 earthquake, *International Journal of Remote S*ensing, *31*(13), 3615–3629, 10.1080/01431161003727754.

Davies, K. and D. M. Baker (1965), Ionospheric effects observed around the time of the Alaskan earthquake of March 28, 1964, *J. Geophys. Res.*, *70*, 2251–2253, doi:10.1029/JZ070i009p02251.

Ding, Z. J. Wu, S. Sun, J. Chen, and P. Ban (2010), The variation of ionosphere on some days before the Wenchuan Earthquake, *Chinese J. Geophy*s, *53*(1), 30–38, doi: 10.3969/j.issn.0001-5733.2010.01.004.

He, Y., D.Yang, J. Qian, and M. Parrot (2011a), Anomaly of the ionospheric electron density close to earthquakes: Case studies of Pu'er and Wenchuan earthquakes, *Earthquake Science*, *24*(6), 549–555.

He, Y., D. Yang, J. Qian, and M. Parrot (2011b), Response of the ionospheric electron density to different types of seismic events, *Nat. Hazards Earth Syst. Sci.*, *11*(8), 2173–2180, doi.org/10.5194/nhess-11-2173-2011.

Hayakawa, M., and O. A. Molchanov (Eds.) (2002), Seismo–Electromagnetics: Lithosphere–Atmosphere–Ionosphere Coupling, *TERRAPUB*, Tokyo.

Hsiao, C. C., J. Y. Liu, K. I. Oyama, N. L. Yen, Y. A. Liou, S. S. Chen, and J. J. Miau (2010), Seismo–ionospheric precursor of the 2008 M_W 7.9 wenchuan earthquake observed by formosat–3/cosmic, *GPS Solutions*, *14*(1), 83–89.

Lefeuvre, F., Rauch, J. L., Lagoutte, D., Berthelier, J. J., and Cerisier, J. C. (1992), Propagation characteristics of dayside low-altitude hiss: case studies, *J. Geophys. Res. Space Phys.*, *97*(A7), 10601–10620.

Lebreton, J.-P., S. Stverak, P. Travnicek, M. Maksimovic, D. Klinge, S. Merikallio, D. Lagoutte, B. Poirier, P.-L. Blelly, Z. Kozacek, and M. Salaquarda (2006), The ISL Langmuir probe experiment processing onboard DEMETER: Scientific objectives, description and first results, *Planetary and Space Science*, *54*(5), 472–486, doi:10.1016/j.pss.2005.10.017.

Lin, J., Y. Wu, F. Zhu, X. Qiao, and Y. Zhou (2009), Wenchuan earthquake ionosphere TEC anomaly detected by GPS, *Chinese J. Geophys.*, *52*(1), 297–300 (in Chinese with English abstract).

Li, M., and M. Parrot (2012), "Real time analysis" of the ion density measured by the satellite DEMETER in relation with the seismic activity, *Nat. Hazards Earth Syst. Sci.*, *12*(9), 2957–2963, doi:10.5194/nhess-12-2957-2012.

Li, M., and M. Parrot (2013), Statistical analysis of an ionospheric parameter as a base for earthquake prediction, *J. Geophys. Res. Space Phys.*, *118*(6), 3731–3739, doi:10.1002/jgra.50313.

Li, M., and M. Parrot (2018), Statistical analysis of the ionospheric ion density recorded by DEMETER in the epicenter areas of earthquakes as well as in their magnetically conjugate point areas, *Adv. Space Res.*, *61*, 974–984, doi:10.1016/j.asr.2017.10.047.

Li, M., H. Tan, and M. Cao (2016), Ionospheric influence on the seismo-telluric current related to electromagnetic signals observed before the Wenchuan M_S 8.0 earthquake, *Solid Earth*, *7*, 1405–1415, doi:10.5194/se-7-1405-2016.

Li, M., J. Lu, X, Zhang, and X, Shen (2019), Indications of Ground-based Electromagnetic Observations to A Possible Lithosphere–Atmosphere–Ionosphere Electromagnetic Coupling before the 12 May 2008 Wenchuan M_S 8.0 Earthquake, *Atmosphere*, *10*(7), 355, doi: 10.3390/atmos10070355.

Liu, C., Y. Guan, X. Zheng, A. Zhang, D. Piero, and Y. Q. Sun (2018), The technology of space plasma in-situ measurement on the China Seismo-Electromagnetic Satellite, *Science China Technological Science*, 10.1007/s11431-018-9345-8.

Liu, J. Y., Y. I. Chen, C. C. Huang, M. Parrot, X. H. Shen, S. A. Pulinets, Q. S. Yang, and Y. Y. Ho (2015), A spatial analysis on seismo–ionospheric anomalies observed by DEMETER during the 2008 *M* 8.0 Wenchuan earthquake, *Journal of Asian Earth Science*s, *114*: S1367912015003399.

Liu, J. Y., Y. I. Chen, C. H. Chen, C. Y. Liu, C. Y. Chen, M. Nishihashi, J. Z. Li, Y. Q. Xia, K. I. Oyama, K. Hattori, and C. H. Lin (2009), Seismoionospheric GPS total electron content anomalies observed before the 12 May 2008 M_W7.9 Wenchuan earthquake, *J. Geophys. Res.*, *114*, A04320, doi:10.1029/2008JA013698.

Liu, J. Y., Y. J. Chuo, S. J. Shan, Y. B. Tsai, S. A. Pulinets, and S. B. Yu (2004), Preearthquake ionospheric anomalies registered by continuous GPS TEC measurements, *Ann. Geophys.*, *22*(5), 1585–1593.

Ma, X., Z. Lin, H. Chen, H. Jin, X. Liu, and L. Jiao (2014), Analysis on ionospheric perturbation of TEC and NmF2 based on GPS and COSMIC data before and after the Wenchuan earthquake, *Chinese J. Geophys.*, *57*(8), 2415–2422, doi:10.6038/cjg20140803 (in Chinese with English abstract).

Maurya, A. K., R. Singh, B. Veenadhari, S. Kumar, and A. K. Singh (2013), Sub–ionospheric very low frequency perturbations associated with the 12 May 2008 M = 7.9 Wenchuan earthquake, *Nat. Hazards Earth Syst. Sci.*, *13*(9), 2331–2336, doi:10.5194/nhess-13-2331-2013.

Molchanov, O. A., and M. Hayakawa (2008), Seismo Electromagnetics and Related Phenomena: History and latest results, *TERRAPUB*, Tokyo, doi.org/10.1016/j.pce.2006.05.001.

Molchanov, O. A., E. Fedorov, A. Schekotov, E. Gordeev, V. Chebrov, V. Surkov, A. Rozhnoi, S. Andreevsky, D. Iudin, S. Yunga, A. Lutikov, M. Hayakawa, and P. F. Biagi (2004), Lithosphere–atmosphere–ionosphere coupling as governing mechanism for preseismic short–term events in atmosphere and ionosphere, *Nat. Hazards Earth Syst. Sci.*, *4* (5/6), 757–767, doi.org/10.5194/nhess-4-757-2004.

Němec, F., O. Santolík, and M. Parrot (2009), Decrease of intensity of ELF/VLF waves observed in the upper ionosphere close to earthquakes: a statistical study, *J. Geophys. Res.*, *114*(A4), A04303, doi.org/10.1029/2008JA013972.

Němec, F., O. Santolík, M. Parrot, and J. J. Berthelier (2008), Spacecraft observations of electromagnetic perturbations connected with seismic activity, *Geophys. Res. Lett.*, *35*(5), L05109, doi.org/10.1029/2007GL032517.

Onishi, T., J. J. Berthelier, and M. Kamogawa (2011), Critical analysis of the electrostatic turbulence enhancements observed by DEMETER over the Sichuan region during the earthquake preparation, *Nat. Hazards Earth Syst. Sci.*, *11*(2), 561–570, doi:10.5194/nhess-11-561-2011.

Parrot, M., and M. Li (2017), Demeter results related to seismic activity, *Ursi Radio Science Bulletin*, *88*(4), 18–25.

Parrot, M. (2011), Statistical analysis of the ion density measured by the satellite DEMETER in relation with the seismic activity, *Earthq. Sci.*, *24*(6), 513–521, doi:10.1007/s11589-011-0813-3.

Parrot, M. (2012), Statistical analysis of automatically detected ion density variations recorded by DEMETER and their relation to seismic activity, *Ann. Geophys.*, *55*(1), 149–155, doi:10.4401/ag-5270.

Parrot, M., J. J. Berthelier, J. P. Lebreton, J. A. Sauvaud, O. Santolík, and J. Blecki (2006), Examples of unusual ionospheric observations made by the DEMETER satellite over seismic regions, *Physics and Chemistry of the Earth*, *31*, 486–495, doi:10.1016/j.pce.2006.02.011.

Píša, D., F. Němec, M. Parrot, and O. Santolík (2012), Attenuation of electromagnetic waves at the frequency ~1.7 kHz in the upper ionosphere observed by the DEMETER satellite in the vicinity of earthquakes, *Ann. Geophys.*, *55*(1), 157–163, doi:10.4401/ag-5276.

Píša, D., F. Němec, O. Santolík, M. Parrot, and M. Rycroft (2013), Additional attenuation of natural VLF electromagnetic waves observed by the DEMETER spacecraft resulting from preseismic activity, *J. Geophys. Res.*, *118*(8), 5286–5295, doi:10.1002/jgra.50469.

Pulinets, S. A., A. D. Legen'ka, and V. A. Alekseev (1994), Pre–earthquakes effects and their possible mechanisms, In: Dusty and Dirty Plasmas, Noise and Chaos in Space and in the Laboratory, *Plenum Publishing*, New York, 545–557.

Pulinets, S. A., and D. Ouzounov(2011), Lithosphere–Atmosphere–Ionosphere Coupling (LAIC) model, An unified concept for earthquake precursors validation, *J. Asian Earth Sci.*, *41*, 371–382, doi:10.1016/j.jseaes.2010.03.005.

Pulinets, S. A., K. A. Boyarchuk, V. V. Hegai, V. P. Kim, and A. M. Lomonosov (2000), Quasielectrostatic model of atmosphere–thermosphere–ionosphere coupling, *Adv. Space Res*, *26*, 1209–1218, doi.org/10.1016/s0273-1177(99)01223-5.

Pulinets, S. A., V. A. Alekseev, A. D. Legen'ka, and V. V. Khegai (1997), Radon and metallic aerosols emanation before strong earthquakes and their role in atmosphere and ionosphere modification, *Adv. Space Res.*, *20*, 2173–2176, doi.org/ 10.1016/s0273-1177(97)00666-2.

Pulinets, S. A., V. G. Bondur, M. N. Tsidilina, M. V. Gaponova (2009), Verification of the concept of seismoionospheric coupling under quiet heliogeomagnetic conditions, using the Wenchuan (China) earthquake of May 12, 2008, as an example, *Geomagnetism and Aeronomy*, *50*(2), 231–242.

Pulinets, S. A., A. D. Legen, T. V. Gaivoronskaya, and V. K. Depuev (2003), Main phenomenological features of ionospheric precursors of strong earthquakes, *J. Atmos. Sol.-Terr. Phys.*, *65*, 1337–1347.

Ryu, K., M. Parrot, S. G. Kim, K. S. Jeong, J. S. Chae, S. Pulinets, K. I. Oyama (2014), Suspected seismo–ionospheric coupling observed by satellite measurements and GPS TEC related to the *M*7.9 Wenchuan earthquake of 12 May 2008, *J. Geophys. Res. Space Physics.*, *119*(10), 305–323. doi:10.1002/2014JA020613.

Sarkar, S., and A. K. Gwal (2010), Satellite monitoring of anomalous effects in the ionosphere related to the great Wenchuan earthquake of May 12, 2008, *Nat. Hazards Earth Syst. Sci.*, *55*(2), 321–332, doi:10.1007/s11069-010-9530-9.

Savitzky, A. and M. J. E. Golay (1964), Smoothing and differentiation of data by simplified least squares procedures, *Anal. Chem.*, *36*, 1627–1639.

Shen, X., X. Zhang, S. Yuan, L. Wang, J. Cao, J. Huang, X. Zhu, P. Piergiorgio, and J. P. Dai (2018), The state-of-the-art of the China Seismo-Electromagnetic Satellite mission, *Sci. China Technol. Sci.*, *61*(5), 634–642, doi:10.1007/s11431-018-9242-0.

Silina, A. S., E. V. Liperovskaya, V. A. Liperovsky, and C.-V. Meister (2001), Ionospheric phenomena before strong earthquakes, *Nat. Hazards Earth Syst. Sci.*, *1*(3), 113–118, doi:10.5194/nhess-1-113-2001.

Sorokin, V., V. Chemyrev, and M. Hayakawa (2015), Electrodynamic Coupling of Lithosphere–Atmosphere–Ionosphere of the Earth, *Nova Science Pub. Inc*, doi: 10.1016/j.jseaes.2010.03.005.

Stangl, G., and M. Y. Boudjada (2011), Investigation of TEC and VLF space measurements associated to L'Aquila (Italy) earthquakes, *Nat. Hazards Earth Syst. Sci.*, *11*(4), 1019–1024, doi: 10.5194/nhess-11-1019-2011.

Sun, Y., K.–I. Oyama, J. Y. Liu, H. K. Jhuang, and C. Z. Cheng (2011), The neutral temperature in the ionospheric dynamo region and the ionospheric F region density during Wenchuan and Pingtung Doublet earthquakes, *Nat. Hazards Earth Syst. Sci.*, *11*(6), 1759–1768, doi:10.5194/nhess-11-1759-2011.

Walker, S. N., V. Kadirkamanathan, and O. A. Pokhotelov (2013), Changes in the ultra–low frequency wave field during the precursor phase to the Sichuan earthquake: DEMETER observations, *Ann. Geophys.*, *31*, 1597–1603, doi:10.5194/angeo-31-1597-2013.

Wan, J., F. Wang, X. Shan, and X. Yan (2012), Preliminary application of energetic particle on DEMETER Satellite in Wenchuan earthquake, *Progress in Geophysics*, *27*(6), 2279–2288 (in Chinese with English abstract).

Xu, T., Y. Hu, J. Wu, Z. Wu, Y. Suo, and J. Feng (2010a), Giant disturbance in the ionospheric F2 region prior to the *M* 8.0 Wenchuan earthquake on 12 May 2008, *Annales Geophysicae*, *28*, 1533–1538, doi:10.5194/angeo-28-1533-2010.

Xu, T., Y. Hu, Wu, Z. Wu, Y. Suo, J. Feng, and C. Huang (2010b), Abnormal perturbations in the ionospheric F2 region before Wenchuan earthquake on 12 May 2008, *Science in China Series D: Earth Sciences*, *53*(11), 1671–1674, doi: 10. 1007/s11430-010-4046-4.

Xu, T., J. Wu, Z. Zhao, Y. Liu, S. He, J. Li, Z. Wu, and Y. Hu (2011), Brief communication "Monitoring ionospheric variations before earthquakes using the vertical and oblique sounding network over China", *Nat. Hazards Earth Syst. Sci.*, *11*(4), 1083–1089, doi:10.5194/nhess-11-1083-2011.

Yan, R., M. Parrot, and J. L. Pinçon (2017), Statistical study on variations of the ionospheric ion density observed by DEMETER and related to seismic activities, *J. Geophys. Res.*, *122*(12), 12421–12429, doi:10.1002/2017JA024623.

Yan, R., Y. Guan, X. Shen, J. Huang, X. Zhang, C. Liu, and D. Liu (2018), The Langmuir Probe onboard CSES: data inversion analysis method and first results, *Earth Planet. Phys.*, *2*, 479–488, doi: 10.26464/epp2018046.

Yan, X., X. Shan, J. Cao, J. Tang, and F. Wang (2012), Seismoionospheric anomalies observed before the Wenchuan earthquake using GPS and DEMETER data, *Seismology and Geology*, *34*(1), 160–171, doi: 10.3969 /j. issn. 0253–4967. 2012. 01. 015.

Yu, T. T. Mao, Y. G. Wang, and J. S. Wang (2009), Study of the ionospheric anomaly before the Wenchuan earthquake, Chinese Science Bulletin, *54*(6), 1086–1092, doi: CNKI:SUN:JXTW.0.2009-06-026 (in Chinese with English abstract).

Zeng, Z., B. Zhang, G. Fang, D. Wang, and H. Yin (2009), The analysis of ionospheric variations before Wenchuan earthquake with DEMETER data, *Chinese J. Geophys.*, *52*(1), 11–19 (in Chinese with English abstract).

Zhang, X., X. Shen, J. Liu, X. Ouyang, J. Qian, and S. Zhao (2009a), Analysis of ionospheric plasma perturbations before Wenchuan earthquake, *Nat. Hazards Earth Syst. Sci.*, *9*(4), 1259–1266,10.5194/nhess-9-1259-2009.

Zhang, X., X. Shen, X. Ouyang, J. Cai, J. Huang, J. Liu , and S. Zhao (2009b), Ionosphere VLF electric field anomalies before Wenchuan *M* 8 earthquake, *Chinese Journal of Radio Science*, *24*(6), 1024–1032 (in Chinese with English abstract).

Zhang, X., C. Fidani, J. Huang, X. Shen, Z. Zeren, and J. Qian (2013), Burst increases of precipitating electrons recorded by the DEMETER satellite before strong earthquakes, *Nat. Hazards Earth Syst. Sci.*, *13*(1), 197–209, doi:10.5194/nhess-13-197-2013.

Zhao, B., M. Wang, T. Yu, G. Xu, W. Wan, and L. Liu (2010), Ionospheric total electron content variations prior to the 2008 Wenchuan Earthquake, *International Journal of Remote Sensing*, *31*(13), 3545–3557, doi: 10.1080/01431161003727622.

Zhao, B., T. Yu, M. Wang, W. Wan, J. Lei, L. Liu, and B. Ning (2008), Is an unusual large enhancement of ionospheric electron density linked with the 2008 great Wenchuan earthquake? *J. Geophys. Res.*, *113*, A11304, doi:10.1029/2008JA013613.

Zhu, F., Y. Wu, J. Lin, Y. Zhou, J. Xiong, J. Yang (2009), Anomalous response of ionospheric VTEC before the Wenchuan earthquake, *Acta Seismologica Sinica*, *31*(2), 180–187.